Received Date : 02-Jan-2014

Revised Date : 08-Jul-2014

Accepted Date : 12-Jul-2014

Article type : Research Article

Molecular Modeling, Synthesis and Biological Evaluation of *N*-Heteroaryl Compounds as Reverse Transcriptase Inhibitors against HIV-1

Anuradha Singh[1], Dipti Yadav[1], Madhu Yadav[1], Ashwini Dhamanage[2], Smita Kulkarni[2, $] and Ramendra K. Singh[1, $,*]

[1] *Nucleic Acids and Antiviral Research Laboratory, Department of Chemistry, University of Allahabad, Allahabad-211002, India*

[2]*National AIDS Research Institute, Pune, India*

$Equal contribution

[*]*Corresponding author: Ramendra K. Singh,* rksinghsrk@gmail.com, Telefax. No. +91-532-2461005

Abstract

Different *N*-heteroaryl compounds bearing pyrimidine and benzimidazole moieties have been designed *in silico* using Discovery studio 2.5 software, synthesized and evaluated for their inhibitory activity as reverse transcriptase inhibitors against HIV-1 replication using laboratory adapted strains HIV-1_{IIIB} (X4, subtype B) and HIV-1_{Ada5} (R5, subtype B), and the primary isolates HIV-1_{UG070} (X4, subtype D) and HIV-1_{VB59} (R5, subtype C). Cell based assay showed that compounds were active at 1.394 µM concentrations (Selectivity Index: 1.29-38.39). The studies on structure–activity relationship clearly suggested anti-HIV activity of pyrimidine and benzimidazole derivatives and these findings were consistent with the *in vitro* cell based experimental data. The results of molecular modeling and docking confirmed that all compounds assumed a butterfly like conformation and showed H-bond, 'π-π' and 'π- +' and hydrophobic interactions within flexible non-nucleoside inhibitor binding pocket of HIV-1 reverse transcriptase, similar to known non-nucleoside reverse transcriptase inhibitors, such as nevirapine. In view of the results obtained, it can be said that the chemical skeletons of *N, N'-bis-(pyridin-2-yl)-succinamide (***14** and **15**) and *1, 4-bis-benzoimidazol-1-yl-butane-1, 4-dione* (**16** and **17**) may be used for developing potent inhibitors of HIV-1 replication, with suitable structure/pharmacophore modifications.

Key Words: HIV-1 reverse transcriptase, anti-HIV activity, docking, TZM-bl cell lines

This article has been accepted for publication and undergone full peer review but has not been through the copyediting, typesetting, pagination and proofreading process which may lead to differences between this version and the Version of Record. Please cite this article as an 'Accepted Article', doi: 10.1111/cbdd.12397

Introduction

Acquired immunodeficiency syndrome (AIDS) continues to be a threat to human life since 1983 and presently around 35.3 million people are living with HIV, its etiological agent (1). Significant progress has been made in developing therapeutic agents to control HIV replication and introduction of combination therapy, highly active antiretroviral therapy (HAART) has delayed the onset of AIDS and slowed down its global epidemic and drastically prolonged the life expectancy of HIV-1 positive patients. However, the imminent development of drug resistance and the toxic side effects associated with HAART prompt continuous efforts toward the discovery of new therapeutics with unique mechanism of action. Though current combination therapy has provided an improved quality of life, researchers are pursuing development of new anti-HIV drugs because of the problems associated with current anti-retroviral therapy (2-4).

Currently, five classes of FDA approved antiretroviral agents exist, viz. reverse transcriptase inhibitors (RTIs), protease inhibitors (PIs), integrase inhibitors (IIs), fusion inhibitors (FIs) and chemokine receptor antagonists (CRAs). The target enzyme reverse transcriptase (RT), focused in present study, plays a crucial role in the life-cycle of HIV. It has three enzymatic activities - RNA dependent DNA polymerase activity, DNA dependent DNA polymerase activity and RNase-H activity, and is responsible for transformation of HIV genomic ssRNA into dsDNA- the proviral DNA. Thus, HIV-RT has been recognized as a prime target for drug development and several RT inhibitors, like nucleoside reverse transcriptase inhibitors (NRTIs), nucleotide reverse transcriptase inhibitors (NtRTIs) and non-nucleoside reverse transcriptase inhibitors (NNRTIs) have been developed as potential drug molecules against HIV (5).

The NRTIs act as chain terminators and bind at the catalytic site as DNA base mimics (6), while NNRTIs, being small and somewhat nonpolar molecules, exert their biological action on the HIV-RT through interaction within an allosteric non-substrate site, located about 10 Å away from the catalytic site. The interactions within hydrophobic and relatively small cleft known as the non-nucleoside inhibitor binding pocket (NNIBP), cause short- and long range conformational changes (allosteric effect) impending the HIV-RT DNA polymerase activity. The NNRTIs cross the blood brain barrier (BBB) and thus, NNRTIs not only reduce the viral loads across the BBB but also prevent complications, like the onset of AIDS associated dementia (7).

The NNRTIs include a variety of conformationally restrained two and three ring structures with varying degree of flexibility and are specific only for HIV-1 RT because of the presence of a flexible hydrophobic pocket in which NNRTIs can fit. Favourable pharmacokinetic properties, unique antiviral activity, high specificity and wide range of chemically diverse structures make NNRTIs a highly striking ingredient of HAART. The amino acids within the NNRTI binding pocket are prone to mutation, leading to drug resistance and development of HIV variants. Therefore, there is an urgent need to develop novel, highly potent NNRTIs with broad spectrum of antiviral activities.

In the light of the need for new anti-HIV agents and the significant role played by NRTIs and NNRTIs, we focused on developing novel NNRTIs utilizing benzimidazole and pyrimidine moieties having flexible connecting linkages for better adaptability, unlike known NNRTIs having rigid fused systems, to match the hydrophobic nature of the allosteric pocket in HIV RT (8-13). Thus, considering the importance of the benzimidazole and pyrimidine moieties, novel molecules **5-17** with requisite structural features- hydrophilic site flanked by hydrophobic sites, were designed using the DS 2.5 software, synthesized and screened against HIV-1 using *in vitro* cell based model. Molecular docking studies with HIV-1 RT enzyme were used to ascertain behavior of these molecules.

Experimental Procedures

Chemicals were obtained from E. Merck India Ltd, India and Sigma-Aldrich Chemical Company, USA. All solvents were reagent grade, purified and dried before use. Melting points of compounds determined using electro thermal apparatus are uncorrected. Thin layer chromatographic analysis (TLC) was done to monitor the completion of reactions as well as for identification of compounds. The spots were visualized by exposure to iodine vapor and UV light. UV measurements were carried out on Lambda 25 spectrophotometer. ^{1}H NMR and ^{13}C NMR spectra were recorded on DRX 300 MHz instrument using $CDCl_3$ as solvent and TMS as an internal standard. Mass spectra were obtained using a Thermofinnigan TRACE-DSQ Electro Spray Ionization (ESI) mass spectrometer. Elemental analyses were carried out on a Perkin-Elmer 240-C analyzer.

Chemistry

General procedure for synthesis of compounds 5-13

To compound **1a/2a** (1mMol) dissolved in dry acetonitrile and a small amount of pyridine, oxalyl chloride (1.2 mmol) was added drop wise in cold and anhydrous condition. Reaction mixture was stirred at 25°C for 1 h and the solvent removed *in vacuo.* The residual oil dissolved in dry pyridine was used directly in the next step without further purification. To a stirred solution of residual oil in dry pyridine (3 mL) maintained in an ice bath, added drop wise appropriate amine (1 mmol) dissolved in dry acetonitrile (4 mL) and pyridine (1 mL), and stirred the reaction mixture at room temperature. After completion of the reaction, as determined by TLC, the solvent was evaporated under pressure and the residual mass dissolved in ethyl acetate (30 mL). This organic fraction was washed consecutively with 5% $NaHCO_3$ solution (20 mL), brine (20 mL), H_2O (20 mL), dried over anhydrous Na_2SO_4, filtered and evaporated under vacuum (40-50°C) to furnish a solid residue, which was purified by silica-gel column chromatography using hexane–ethyl acetate as eluent.

2-(2, 4-Dioxo-3,4-dihydro-2H-pyrimidin-1-yl)-N-pyridin-2-yl-acetamide ***(5)***

White crystals; yield: 68%; R_f = 0.81; m.p. 200 -202°C ; ^{1}H NMR: δ (ppm) : 8.49 (d, *J* = 11.0 Hz, 1H, C_6-H uracil), 6.07 (d, *J* = 10.8 Hz, 1H, C_5-H uracil), 5.45 (s, 1H, -CH_2), 7.71 (s, 1H, -CONH-), 8.36 (d, *J* = 5.0, 1.2 Hz, 1H, C_6-H pyridine), 7.15 (ddd, *J* = 8.2, 5.1, 1.2 Hz, 1H, C_5-H pyridine), 7.99 (dd, *J* = 8.2, 1.1 Hz, 1H, C_4-H pyridine), 7.86 (td, *J* = 8.0, 1.3 Hz, 1H, C_3-H pyridine); ^{13}C NMR: δ (ppm) 167 (-CONH-), [165 (C_4), 153(C_2), 143 (C_6), 101(C_5) uracil], [153(C_2), 148 (C_6), 135(C_4), 120(C_5), 114(C_3) pyridine], 53 (-CH_2);UV/Vis (EtOH): λmax = 245 nm; MS (EI, 70 eV): *m/z* (%): 247.08 (12.5), 246.00 (100) [*M*+H]+; HRMS-FAB: *m/z* [*M*+H]+ calcd for $C_{11}H_{10}N_4O_3$: 246.08, found: 246.10; Anal. calcd for $C_{11}H_{10}N_4O_3$: C 53.66, H 4.09, N 22.75, found: C 53.68, H 4.08, N 22.78.

N-(5-Bromo-pyridin-2-yl)-2-(2,4-dioxo-3,4-dihydro-2H-pyrimidin-1-yl)-acetamide ***(6)***

Orange solid; yield: 74%; R_f =0.83; m.p. 218-219 °C ; ^{1}H NMR : δ(ppm) : 7.89 (d, *J* = 11.0 Hz, 1H, C_6-H uracil), 5.92 (d, *J* = 10.8 Hz, 1H, C_5-H uracil), 7.71 (s, 1H, -CONH-), 4.42 (s, 2H, -CH_2), 9.26 (d, *J* = 1.3 Hz, 1H, C_6-H pyridine), 8.77 (dd, *J* = 7.9, 1.2 Hz, 1H, C_4-H pyridine), 8.49 (d, *J* = 8.1 Hz,1H, C_3-H pyridine); ^{13}C NMR: δ (ppm) 169 (-CONH-), [165(C_4), 153(C_2), 143 (C_6), 101(C_5) uracil], [152(C_2), 150 (C_6), 142(C_4), 117.5(C_5), 117(C_3) pyridine], 53 (-CH_2); UV/Vis (EtOH): λmax = 248 nm; MS (EI, 70 eV): *m/z* (%): 325.98 (97.3), 323.98 (100) [*M*+H]+; HRMS-FAB: *m/z* [*M*+H]+ calcd for $C_{11}H_9BrN_4O_3$: 323.99, found: 323.98; Anal. calcd for $C_{11}H_9BrN_4O_3$: C 40.64, H 2.79, Br 24.58, N 17.23, found: C 40.62, H 2.78, Br 24.56, N 17.24.

2-(2, 4-Dioxo-3,4-dihydro-2H-pyrimidin-1-yl)-N-(5-nitro-pyridin-2-yl)-acetamide ***(7)***

Brown solid; yield: 77%; R_f = 0.88; m.p. 178-182°C ; ^{1}H NMR : δ(ppm) : 7.92 (d, *J* = 10.8 Hz, 1H, C_6-H uracil), 5.92 (d, *J* = 10.8 Hz, 1H, C_5-H uracil), 7.71 (s, 1H, -CONH-), 4.42 (s, 2H, -CH_2), 9.26 (d, *J* = 1.3 Hz, 1H, C_6-H pyridine), 8.77 (dd, *J* = 7.9, 1.2 Hz, 1H, C_4-H pyridine), 8.49 (d, *J* = 8.1 Hz, 1H, C_3-H pyridine); ^{13}C NMR: δ (ppm) 168.1(-CONH-), [165(C_4), 153(C_2), 143(C_6), 100(C_5) uracil],[159(C_2), 143(C_6), 140(C_5), 134(C_4), 116(C_3) pyridine], 53(-CH_2),UV/Vis (EtOH): λmax = 315 nm, 256 nm; MS (EI, 70 eV): *m/z* (%): 292.07 (14.3), 291.06 (100) [*M*+H]+; HRMS-FAB: *m/z* [*M*+H]+ calcd for $C_{11}H_9N_5O_5$: 291.06, found: 291.08; Anal. calcd for $C_{11}H_9N_5O_5$: C 45.37, H 3.11, N 24.05, found: C 45.35, H 3.10, N 24.02.

2-(5-Methyl-2,4-dioxo-3,4-dihydro-2H-pyrimidin-1-yl)-(N-pyridin-2-yl)-acetamide ***(8)***

White solid; yield: 70%; R_f =0.77; m.p. 221°C ; ^{1}H NMR : δ(ppm) : 8.36 (dd, *J* = 5.0, 1.2 Hz, 1H, C_6-H pyridine), 7.99 (dd, *J* = 8.2, 1.1 Hz, 1H, C_3-H pyridine), 7.86 (td, *J* = 8.0, 1.3 Hz, 1H, C_4-H pyridine), 7.15 (ddd, *J* = 8.2, 5.1, 1.2 Hz, 1H, C_5-H pyridine), 7.71 (s, 1H, -CONH-), 7.62 (q, *J* = 1.0 Hz, 1H, C_6-H thymine), 1.78 (s, 3H, –CH_3 thymine), 4.42 (s, 2H,-CH_2); ^{13}C NMR: δ (ppm) 167.9(-CONH-), [164(C_4), 153(C_2), 138(C_6), 109(C_5), 13.5(–CH_3) thymine], 151(C_2), 148(C_6), 141(C_4), 118(C_5), 113(C_3) pyridine], 53(-CH_2); UV/Vis (EtOH): λmax = 319 nm; MS (EI, 70 eV): *m/z* (%): 261.09 (14.8), 260.09 (100) [*M*+H]+; HRMS-FAB: *m/z* [*M*+H]+ calcd for $C_{12}H_{12}N_4O_3$: 260.09, found: 260.20; Anal. calcd for $C_{12}H_{12}N_4O_3$: C 55.38, H 4.65, N 21,23, found: C 55.36, H 4.64, N 21.22.

N-(5-Bromo-pyridin-2-yl)-2-(5-methyl-2,4-dioxo-3,4-dihydro-2H-pyrimidin-1-yl)-acetamide ***(9)***

Yellow crystals; yield: 75%; R_f = 0.81; m.p. 229-230 °C ; ^{1}H NMR: δ(ppm) : 8.22 (d, *J* = 1.3 Hz, 1H, C_6-H pyridine), 7.97 (dd, *J* = 7.9, 1.2 Hz, 1H, C_4-H pyridine), 8.23 (d, *J* = 8.1 Hz, 1H, C_3-H pyridine), 7.71 (s, 1H, -CONH-), 7.62 (q, *J* = 1.0 Hz, 1H, C_6-H thymine), 1.76 (s, 3H, –CH_3 thymine),4.42 (s, 2H, -CH_2); ^{13}C NMR: δ (ppm) 167.6(-CONH-), [165(C_4), 154(C_2), 135.3(C_6), 109(C_5), 12.5(–CH_3) thymine], [151(C_2), 147.8(C_6), 142(C_4), 115.8(C_5), 115(C_3) pyridine], 53(-CH_2); UV/Vis (EtOH): λmax = 325 nm; MS (EI, 70 eV): *m/z* (%): 340.00 (97.5), 338.00 (100) [*M*+H]+; HRMS-FAB: *m/z* [*M*+H]+ calcd for $C_{12}H_{11}BrN_4O_3$: 338.00, found:

338.10; Anal. calcd for $C_{12}H_{11}BrN_4O_3$: C 42.50, H 3.27, Br 23.56, N 16.52, found: C 42.49, H 3.25, Br 23.57, N 16.53.

2-(5-Methyl-2,4-dioxo-3,4-dihydro-2H-pyrimidin-1-yl)-N-(5-nitro-pyridin-2-yl)-acetamide ***(10)***
Dark brown solid; yield: 80%; R_f = 0.88; m.p. 179-180 °C ; ^{1}H NMR : δ (ppm) : 9.26 (d, *J* = 1.3 Hz, 1H, C_6-H pyridine), 8.77 (dd, *J* = 7.9, 1.2 Hz, 1H, C_4-H pyridine), 8.49 (d, *J* = 8.1 Hz, 1H, C_3-H pyridine), 7.71 (s, 1H, -CONH-), 7.62 (q, *J* = 1.0 Hz, 1H, C_6-H thymine), 1.89 (s, 3H, –CH_3 thymine),4.42 (s, 2H, -CH_2); ^{13}C NMR: δ (ppm) 167.8(-CONH-), [165(C_4), 152(C_2), 133(C_6), 109, (C_5) 13(–CH_3) thymine], [153.4(C_2), 143.2(C_6), 140(C_5), 135(C_4), 112.2(C_3) pyridine], 53(-CH_2);UV/Vis (EtOH): λmax = 315 nm, 256 nm; MS (EI, 70 eV): *m/z* (%): 306.08 (13.7), 305.09 (100) [*M*+H]+; HRMS-FAB: *m/z* [*M*+H]+ calcd for $C_{12}H_{11}N_5O_5$: 305.09, found: 305.12; Anal. calcd for $C_{12}H_{11}N_5O_5$: C 47.22, H 3.63, N 22.94, found: C 47.20, H 3.61, N 22.92.

2-Benzoimidazol-1-yl-N-pyridin-2-yl-acetamide ***(11)***
White solid; yield: 78%; R_f = 0.48 ; m.p. 130 °C ; ^{1}H NMR : δ(ppm) : 8.36 (dd, *J* = 5.0, 1.2 Hz, 1H, C_6-H pyridine), 7.99 (dd, *J* = 8.2, 1.1 Hz, 1H, C_3-H pyridine), 7.86 (td, *J* = 8.0, 1.3 Hz, 1H, C_4-H pyridine), 7.12 (dd, *J* = 8.2, 1.1 Hz, 1H, C_5-H pyridine),7.71 (s, 1H, -CONH-), 7.64 (dd, *J* = 7.4, 1.6 Hz, 2H, $C_{4,7}$ -H benzimidazole), 8.17 (s, 1H, C_2-H benzimidazole), 7.32 – 7.25 (m, 1H, $C_{5,6}$-H benzimidazole), 5.22 (s, 2H, -CH_2); ^{13}C NMR: δ (ppm) 167.7(-CONH-), [141.3(C_2), 137.6(C_8, C_9), 123.5(C_5, C_6), 114.8(C_4, C_7) benzimidazole], [152.2 (C_2), 145.4(C_6), 140.5(C_4), 120.5(C_5), 115(C_3) pyridine], 54.5(-CH2); UV/Vis (EtOH): λmax = 213 nm; MS (EI, 70 eV): *m/z* (%): 253.09 (17.1), 252.11 (100) [*M*+H]+; HRMS-FAB: *m/z* [*M*+H]+ calcd for $C_{14}H_{12}N_4O$: 252.11, found: 252.16; Anal. calcd for $C_{14}H_{12}N_4O$: C 66.65, H 4.79, N 22.21, found: C 66.64, H 4.77, N 22.19.

2-Benzoimidazol-1-yl-N-(5-bromo-pyridin-2-yl) – acetamide ***(12)***
Light brown solid; yield : 78%; R_f =0.48 ; m.p. 247°C ; ^{1}H NMR : δ(ppm) : 8.26 – 8.20 (m, 2H, $C_{3,\ 6}$-H pyridine), 7.97 (dd, *J* = 7.9, 1.3 Hz, 1H, C_4-H pyridine), 8.17 (s, 1H, C_2-H benzimidazole), 7.64 (dd, *J* = 7.4, 1.6 Hz, 2H, $C_{4,7}$ -H benzimidazole), 7.25 (dd, 1H, C_6 -H benzimidazole), 7.20 (td, *J* = 7.5, 1.6 Hz, 1H, C_5 -H benzimidazole), 7.71 (s, 1H,-CONH-), 5.22 (s, 2H,-CH_2); ^{13}C NMR: δ (ppm) 169(-CONH-), [153.5(C_2), 149(C_6), 142(C_4), 117(C_5), 115.9(C_3) pyridine], [142(C_2), 136.6(C_8, C_9), 123.8(C_5, C_6), 114.2(C_4, C_7) benzimidazole], 54.8(-CH2); UV/Vis (EtOH): λmax = 224 nm; MS (EI, 70 eV): *m/z* (%): 332.00 (98.9), 330.10 (100) [*M*+H]+; HRMS-FAB: *m/z* [*M*+H]+ calcd for $C_{14}H_{11}BrN_4O$: 330.10, found: 330.12; Anal. calcd for $C_{14}H_{11}BrN_4O$: C 50.77, H 3.35, Br 24.13, N 16.92, found: C 50.75, H 3.34, N 16.90.

2- Benzoimidazol-1-yl-N-(5-nitro-pyridin-2-yl)-acetamide ***(13)***
Dark yellow solid ; yield : 56%; *Rf* = 0.73; m.p. 138-139 °C ; ^{1}H NMR : δ (ppm) : 9.26 (d, *J* = 1.3 Hz, 1H, C_6-H pyridine), 8.77 (dd, *J* = 7.9, 1.2 Hz, 1H, C_4-H pyridine), 8.49 (d, *J* = 8.1 Hz, 1H, C_3-H pyridine), 7.71 (s, 1H, -CONH-), 8.17 (s, 1H, C_2-H benzimidazole), 7.64 (dd, *J* = 7.4, 1.6 Hz, 2H, $C_{4,7}$ -H benzimidazole), 7.25 (m, 1H, C_6 -H benzimidazole), 7.20 (td, *J* = 7.5, 1.6 Hz, 1H, C_5 -H benzimidazole), 5.22 (s, 2H, -CH_2); ^{13}C NMR: δ (ppm) 169(-CONH-), [157(C_2), 143(C_6), 140(C_5), 134(C_4), 114(C_3) pyridine],[141.3(C_2), 136.9(C_8, C_9), 123.2(C_5, C_6), 115.2(C_4, C_7) benzimidazole], 54.8(-CH_2); UV/Vis (EtOH): λmax = 210 nm; MS (EI, 70 eV): *m/z* (%): 298.11 (17.7), 297.10 (100) [*M*+H]+; HRMS-FAB: *m/z* [*M*+H]+ calcd for $C_{14}H_{11}N_5O_3$ 297.10, found: 297.12; Anal. calcd for $C_{14}H_{11}N_5O_3$: C 56.56, H 3.73, N 23.56, found: C 56.54, H 3.72, N 23.55.

General procedure for synthesis of compounds **14-17**
3a (2.5 mmol, in the case of compounds **14-15**)**/ 4a** (2.5 mmol, in the case of compounds **16-17**) was suspended in dry pyridine (4 mL) in a 100 mL round bottomed flask and added succinoyl chloride (1 mmol) and stirred the reaction mixture for 4 h. The solvent was removed *in vacuo* and the resulting material was partitioned between aqueous $NaHCO_3$ solution and DCM. The organic layer was dried over anhydrous Na_2SO_4, filtered, concentrated *in vacuo* and the product was crystallized using a mixture of ethyl acetate and hexane.

N,N'-Bis-(5-bromo-pyridin-2-yl)-succinamide ***(14)***
Light brown crystals; yield: 75%; R_f = 0.81; m.p. 137°C; ^{1}H NMR : δ (ppm): 2.45 (s, 2H,-CH_2), 8.26 – 8.20 (m, 2H, $C_{3\text{-}6}$ -H pyridine), 7.97 (dd, *J* = 7.9, 1.3 Hz, 1H, C_4-H pyridine); ^{13}C NMR: δ (ppm) 172.4(-CONH-), [152.2 (C_2), 149.4(C_6), 140.5(C_4), 115.5(C_5), 115(C_3) pyridine], 30.8(-CH_2); UV/Vis (EtOH): λmax = 280 nm; MS (EI, 70 eV): *m/z* (%): 429.80 (50.0), 427.80 (100) [*M*+H]+; HRMS-FAB: *m/z* [*M*+H]+ calcd for $C_{14}H_{12}Br_2N_4O_2$: 427.80, found: 427.82; Anal. calcd for $C_{14}H_{12}Br_2N_4O_2$: C 39.28, H 2.83, Br 37.33, N 13.09, found: C 39.26, H 2.80, Br 37.31, N 13.08.

N,N'-Bis-(5-nitro-pyridin-2-yl)-succinamide ***(15)***
white crystals; yield: 85%; R_f = 0.67; m.p. 147°C; ^{1}H NMR : δ (ppm): 2.45 (s, 2H,-CH_2), 9.26 (d, *J* = 1.3 Hz, 1H, C_6 -H pyridine), 8.77 (dd, *J* = 7.9, 1.2 Hz, 1H, C_4-H pyridine), 8.49 (d, *J* = 8.1 Hz, 1H, C_3-H pyridine); ^{13}C

NMR: δ (ppm) 172.4(-CONH-), [158.2 (C_2), 142.4(C_6), 140.5(C_5), 132.5(C_5), 115(C_3) pyridine], 30.2(-CH_2); UV/Vis (EtOH): λmax = 294 nm; MS (EI, 70 eV): *m/z* (%): 361.10 (18.2), 360.10 (100) [*M*+H]+; HRMS-FAB: *m/z* [*M*+H]+ calcd for $C_{14}H_{12}N_6O_6$: 360.10, found: 360.12; Anal. calcd for $C_{14}H_{12}N_6O_6$: C 46.67, H 3.36, N 23.33, found: C 46.65, H 3.34, N 23.30.

1, 4-Bis-benzoimidazol-1-yl-butane-1, 4-dione ***(16)***
Brown solid; yield: 80%; R_f = 0.66; m.p. 145-146 °C; ^{1}H NMR : δ (ppm): 8.08 (s, 1H, C_2-H benzimidazole), 7.56 (ddd, *J* = 7.0, 4.9, 1.7 Hz, 2H, $C_{4,7}$-H benzimidazole), 7.29 – 7.17 (m, 2H, $C_{5,6}$-H benzimidazole), 2.73 (s, 2H, -CH_2); ^{13}C NMR: δ (ppm) 202(-CONH-), [141.3(C_2), 137.6(C_8, C_9), 123.5(C_5, C_6), 114.8(C_4, C_7) benzimidazole], 26.8(-CH_2); UV/Vis (EtOH): λmax = 267 nm; MS (EI, 70 eV): *m/z* (%): 319.10 (21.8), 318.12 (100) [*M*+H]+; HRMS-FAB: *m/z* [*M*+H]+ calcd for $C_{18}H_{14}N_4O_2$: 318.12, found: 318.14; Anal. calcd for $C_{18}H_{14}N_4O_2$: C 67.91, H 4.43, N 17.60, found: C 67.89, H 4.41, N 17.58.

1-Bis-(4-nitro-benzoimidazol-1-yl)-butane-1, 4-dione ***(17)***
Yellow solid; yield: 60%; R_f = 0.58; m.p. 154-156 °C; ^{1}H NMR : δ (ppm): 8.14 (dd, *J* = 7.5, 1.5 Hz, 1H, C_7-H benzimidazole), 8.08 (s, 1H, C_2-H benzimidazole), 7.95 (dd, *J* = 7.5, 1.5 Hz, 1H, C_5-H benzimidazole), 7.49 (t, *J* = 7.4 Hz, 1H, C_6-H benzimidazole); ^{13}C NMR: δ (ppm) ^{13}C NMR: δ (ppm) 202(-CONH-), [142.3(C_2), 138.6(C_8), 134.8(C_4), 132.7(C_9), 122.9(C_6), 120.8(C_7), 118.5(C_5) benzimidazole], 26.9(-CH_2); UV/Vis (EtOH): λmax = 252 nm; MS (EI, 70 eV): *m/z* (%): 409.10 (22.7), 408.10 (100) [*M*+H]+; HRMS-FAB: *m/z* [*M*+H]+ calcd for $C_{18}H_{12}N_6O_6$: 408.10, found: 408.12; Anal. calcd for $C_{18}H_{12}N_6O_6$: C 52.95, H 2.96, N 20.58, found: C 52.94, H 2.94, N 20.56.

In vitro **Anti-HIV-1 assay**
In vitro anti-HIV assay was carried out using published procedure (28).

Cell lines
TZM-bl cell line was used for primary screening of all compounds. TZM-bl cells were obtained from NIH AIDS Research and Reference Reagent Programme (NIH ARRRP), USA. These are genetically engineered HeLa cells, which have been modified to express different receptors, like CD4, CXCR4, and CCR5 and contain Tat-responsive reporter genes for firefly luciferase (Luc) and Escherichia coli β-galactosidase under regulatory control of an HIV-1 LTR. The cells were maintained in Dulbecco's Modified Eagle's Medium DMEM (Gibco, USA) containing 10% heat inactivated fetal bovine serum (Morgate, Australia), HEPES (Gibco, USA), penicillin, streptomycin (Gibco, USA) and gentamicin (Sigma, USA) and the cultures were incubated at 37^{0}C in a humidified 5% CO_2 atmosphere.

Viral Stocks
The laboratory adapted strains HIV-1_{IIIB} (X4, subtype B), HIV-1_{Ada5} (R5, subtype B) and the primary isolates HIV-1_{UG070} (X4, subtype D) were obtained from NIH ARRRP, whereas R5 tropic isolate HIV-1_{VB59} (subtype C) was an Indian isolate from the National AIDS Research Institute, Pune. The viruses were grown in PHA-P activated (Sigma Aldrich, USA) peripheral blood mononuclear cells (PBMC) derived from healthy donors. The virus production was quantified in cell culture supernatants by HIV-1 p24 antigen detection kit (Vironostika HIV-1 Antigen, Biomerieux, Netherlands). Aliquots of cell-free culture viral supernatants, stored at -70^{o}C were used as the viral stocks and the 50% tissue culture infectivity dose ($TCID_{50}$) of each isolate was determined in the appropriate cell line by using the Spearman Karber formula.

Cytotoxicity Assay
The TZM-bl cells (1×10^4/well/100µL medium) were seeded and the plate was incubated overnight at 37^{o}C with 5% CO_2. On the next day, the medium was replaced with 100 µL of two fold dilution series of each compound and was incubated further. After 48 h, the cell viability was determined using MTT assay (3-[4,5-dimethylthiazol-2-yl]-2,5-diphenyltetrazolium bromide, Sigma, USA). In this assay, the measured absorbance is proportional to the viable cell number and inversely to the degree of cytotoxicity. Three independent assays using quadruplicate measurements were carried out for each compound and the mean CC_{50} value was calculated.

Cell associated Anti-HIV-1 assay
The TZM-bl cells (1×10^4/well/100µL media) were seeded in a 96-well plate and incubated overnight at 37^{o}C with 5% CO_2. On the subsequent day, the cells were infected with 400 $TCID_{50}$ HIV-1 stock and incubated for 2 h at 37^{o}C with 5% CO_2. Serial dilutions of each compound showing more than 50% viability were then added in duplicate onto the cells. The anti-HIV activity was determined after 48 h of incubation by measuring the relative luminescence units (RLU) using the Britelite Plus substrate (Perkin Elmer). In this assay, RLU is directly

proportional to the number of virus particles and inversely to the percent of inhibition. The concentration showing 50% inhibition (IC_{50}) was determined using Luc software. The results were interpreted as mean of two independent assays. Nevirapine was used as a positive control.

Molecular modeling

The computational studies were carried out with the X-ray crystal structure of HIV-1 RT complexed with a ligand (PDB: ID 3E01). All computational studies were carried out using Discovery Studio 2.5 (DS 2.5; Accelrys Ltd., USA) obtained through Apsara Innovations Pvt Ltd, Bangalore, India) on an Intel Pentium 2.99 GHz processor, 1.99 GB RAM with Windows XP professional version 2002 operating system. Receptor from the target protein (PDB: ID 3E01) and ligands were prepared according to the published procedure (8).

Receptor set up

The target protein [PDB: ID 3E01] was taken, the ligand extracted, the missing hydrogens added, and their positions optimized using the all-atom CHARMm forcefield and the Adopted Basis set Newton Raphson (ABNR) method available in DS 2.5 protocol until the root mean square (r.m.s.) gradient was less than 0.05 kcal/mol/Å. The minimized protein was defined as the 'receptor' using the binding site module of DS 2.5. The binding site was defined from the volume of ligand method, which was modified to accommodate all important interacting residues in the active site of HIV-1 RT. The Input Site Sphere was defined over the binding site, with a radius of 5Å from the center of the binding site. The protein, thus characterized, was taken as the target receptor for the docking procedure. Minimization was performed to relax these newly added hydrogen atoms by fixing all other non-hydrogen atoms. The minimized structure of the protein was used in docking simulations.

Ligand set up

Using the built-and-edit module of DS 2.5, various ligands were built; all-atom CHARMm forcefield parameterization was assigned and then minimized using the ABNR method. A conformational search of the ligand was carried out using a stimulated annealing molecular dynamics (MD) approach. The ligand was heated to a temperature of 700 K and then annealed to 200 K. Thirty such cycles were carried out. The transformation obtained at the end of each cycle was further subjected to local energy minimization, using the ABNR method. The 30 energy-minimized structures were then superimposed and the lowest energy conformation occurring in the major cluster was taken to be the most probable conformation.

Docking and scoring

Molecular docking is a computational method used to predict the binding of the ligand to the receptor binding site by varying position and conformation of the ligand. Binding mode of inhibitors can be explored by using the LigandFit docking protocol (14, 15). LigandFit algorithm performed a shape comparison filter with a Monte Carlo conformational search (bond lengths and bond angles fixed and only the rotatable bonds were allowed to rotate freely) to generate docked poses parallel to the shape of the binding site. Dreiding forcefield, grid-based calculated interaction energy, is used to refine these poses by rigid body minimization. The receptor protein was fixed during docking. The docked poses were further minimized by using all-atom CHARMm forcefield and smart minimizer method until the r.m.s gradient for potential energy was less than 0.001 kcal mol^{-1} $Å^{-1}$ and evaluated with a set of scoring functions **(Table 2)**. The atoms of ligand and the side chains of the residues of the receptor within 5 Å from the center of the binding site were kept flexible during minimization. The LUDI III score was used to score the refined poses. The ligand pose, which corresponded to the highest LUDI III score was taken as the best docked pose Furthermore, determination of binding energy to assess the binding affinity of ligands for receptor was calculated by employing highest stable ligand-receptor complex through the protocol 'Calculate Binding Energies' within DS 2.5 using the default settings [16-20].

Validation of the docking methodology

Docking was first tested on known inhibitor - nevirapine, which was docked in the allosteric binding site of HIV-1 RT, after extracting the ligand from the crystal structure. A deviation was observed in the conformation of the docked ligand on superimposition with nevirapine. Table 1 showed the docked inhibitors with the HIV-1 RT. This is in good agreement with the observed values for nevirapine. The root mean square deviation (RMSD) of the best docked poses of the molecules reported herein was less than 2 Å, which was supposed to be an appropriate condition for developing NNRTIs. Two structures overlapped very well with positional RMSD of 1.2. The docked pose having the highest LUDI III score gave the least RMSD with respect to the crystal conformation for both the ligands. The analysis of the results showed a sound validation of the docking and scoring methodology used in this study and the ligand as a whole moved into a more stable position with a much lower docked energy.

Calculation of H-acceptors, H-donors, TPSA and logP values

H-acceptors, H-donors and TPSA were calculated using Molinspiration software and logP values using ChemDraw software.

Results and Discussion

Chemistry

The newly designed *N*-heteroaryl compounds **5-13** were synthesized via different routes detailed in **Scheme 1**. The starting intermediates **1a (**uracil *N* (1)-acetic acid), **1b (**thymine *N* (1)-acetic acid) and **1c (**benzimidazole *N* (1)-acetic acid) were prepared according to the published procedure (21). To a solution of compound **1a** or **(1b** or **1c)** in dry acetonitrile containing pyridine as a catalyst, was added oxalyl chloride drop wise in cold and anhydrous condition. The reaction mixture was stirred for 1h and the extra oxalyl chloride removed under pressure. The residual oil dissolved in dry pyridine was used directly in the next step without further purification. To a stirred solution of residual oil in dry pyridine maintained in an ice bath, added drop wise appropriate amine dissolved in dry acetonitrile and pyridine, and stirred the reaction mixture at room temperature. The derivatives **14-15** were synthesized using 2-amino-5-substituted-pyridine and succinoyl chloride (**Scheme 2**). Similarly, other bases, viz. benzimidazole and 4-nitro-benzimidazole were also reacted with succinoyl chloride to get the products **16** and **17**. The reaction mixture was treated with sodium bicarbonate solution and extracted with dichloromethane. Organic extract was dried over anhydrous sodium sulfate and concentrated under reduced pressure. Finally, the pure product was separated by silica-gel column chromatography using ethyl acetate and hexane (22-23).

Molecular docking analysis

We have examined sixty *N*-heteroaryl compounds to develop some potent and selective inhibitors of HIV-1 RT by using *in silico* structure-based approach. On the basis of preliminary *in silico* investigations, we selected thirteen promising molecules for further studies. All compounds have amide linkages. The presence of a C=O dipole and a small N-C dipole allowed these molecules to function as H-bond acceptors as well as H-bond donors. Since these molecules have both H-donor and H-acceptor sites, they can ionize at an appropriate pH to further enhance their solubility. Thus, these molecules have potential to internalize better in cells. Some physically significant descriptors and pharmaceutically relevant properties of designed molecules, like molecular weight, H-bond donors, H-bond acceptors, logP (octanol/water) have been analysed on the basis of Lipinski's rule of five and the results are summarized in Table 1. Molecules showing more than one type of violations are supposed to have problems with bioavailability, hence rejected. In the present study (**Table 1**), all ligands showed the allowed values for the properties analysed and exhibited drug-like characteristics based on Lipinski's rule of five.

Molecular docking is frequently used tool in computer-assisted drug discovery. It is used to predict the preferred orientation, affinity and activity of small molecules into the active site of target protein through a process involving a series of steps **(24).** Docking results have been discussed using the parameters, like hydrogen bond, non-bonded 'π-π' and 'π-+' interactions as they help stabilize and strengthen receptor-ligand complexes. The 'π-π' and 'π- +' interactions are non-covalent interactions and play crucial role in protein-ligand recognition. According to Gallivan and Dougherty, the effective distance for 'π- +' interactions necessary for receptor-ligand recognition should fall below 6Å (25) and values observed for all compounds **(5-17)** are well below this range.

Docking of molecules 5-17 using DS 2.5 into the allosteric site of target protein [PDB: ID 3E01] generated the plausible binding conformations with the corresponding Ludi_3 values. The cluster analysis revealed a predominant orientation of the ligands within the binding pocket of active site and the conformation with the highest Ludi_3 score for each molecule was chosen for further analysis. In order to derive maximum information about interactive forces for receptor-ligand interaction, the entire set of molecules were rigorously docked into the allosteric site of HIV-1 RT, using the same protocol and analysed through above mentioned parameters and results presented in **Table 2**

Visual inspection of the minimized complexes of inhibitors with HIV-1 RT showed the requisite electronic and hydrophobic interactions, suitable for providing stability of a certain level to the protein-ligand complex, between the enzyme and the ligands. These derivatives, like the other NNRTIs, adopted a common "butterfly" conformation. **(Figure 1)** However, there are important differences in their conformations and specific positioning within the NNIBP. The molecules formed one to three H-bonds with various amino acids (Lys 101, Lys 103, His 235, Pro 236 and Tyr 318) present in the NNRTI binding site of HIV-1 RT.

Notably, the NNRTI binding pocket is largely hydrophobic and few H-bonds are accommodated. For the pyrimidine based RTIs, the H-bond between the N(3)H of the inhibitor and the backbone carbonyl group of Lys101 represented the major hydrophilic interaction. To maximize hydrophobic interactions throughout the binding pocket, this H-bond not only contributed to the binding affinity but also served as an anchor for the inhibitor to adopt optimized conformation (26).

In compound **5,** uracil ring pointed towards aromatic amino acid residue within NNBP showed π interaction with Tyr 181 (4.4 Å) and heteroaryl ring showed π interaction with Tyr 318 (4.5 Å), but did not form any H-bond. In the case of compounds **6** and **7,** the C=O portion of the uracil ring formed H-bonds with Lys 103 and Val 106 and the pyridine ring containing bromo and nitro group did not participate in any interaction and no H-bond formation occurred. In compound **8,** the C=O portion of the thymine ring formed H-bond with Lys 103 (2.8 Å) and the ring showed π interaction with Phe 227 (5.2 Å). In compound **9,** C=O portion of the thymine ring formed one H-bond with Val 106 (3.2 Å) and showed π interaction with Phe 227 (5.4 Å) and the amide linkage formed H-bonds with Tyr 318 (2.9 Å). In compound **10,** the thymine ring formed two H-bonds, the first between Lys 103 and C=O portion of thymine ring and the second bond (3.1 Å) between Lys 103 and –NH group of ring . Further, the -NO_2 group formed another H-bond with side chain of Tyr 181(3.1 Å). In compound **11,** the benzimidazole nucleus showed two π interactions with Tyr 181 (4.4 Å and 5.3 Å). In compounds **12** and **13,** the amide linkage formed one H-bond with Lys 103 (2.8 Å each) **(Figure 2 and Figure 3)**. In compound **14,** the amide linkage formed one H-bond with Lys 103. Similarly, in compound **15,** the amide linkage formed one H-bond with Lys 103 (3.1 Å) and the NO_2 group showed two π- cation interactions with Trp 229 (6 Å and 5 Å).

Compounds **16 and 17** did not show any interaction with HIV RT. However, surprisingly, their total interaction energy was comparable or a bit higher than the reference and other compounds **(Table 2)**. This indicated a unique structure–activity relationship that depended on LogP and total polar surface area (TPSA) of the compounds and, in turn, on hydrophobicity **(Figure 2).** Compounds **16 and 17** had higher LogP values and showed more hydrophobic character. The hydrophobic effect arises due to the interaction of non polar atoms on surrounding water molecules and the magnitude of the hydrophobic effect is proportional to the TPSA of the non polar atoms that the molecule contains, as shown by **Table 2** (27). Thus, it can be inferred that in the absence of H-bond, 'π-π' and 'π- +' interactions with key amino acid residue of NNBP, it is the hydrophobic interaction that stabilizes the HIVRT-ligand, which depends on LogP and TPSA values for that compound.

Different groups at the C-5 of the heteroaryl moieties also influenced the inhibitory activity of the compounds. Analogs having nitro group at the termini exhibited better anti-HIV activity (compounds 7**, 10, 15, 16 and 17**) however, the compound having Br atom at the terminus (compound **14**) showed the highest activity.

Anti-HIV evaluation

The compounds **5**–**13** and **14-17** presented in this study were evaluated for their anti-HIV-1 activity using cell based assays. The results, expressed as EC_{50}, CC_{50} and the selectivity index (SI), are summarized in **Table 3**. In the cell based assay, the compounds **14**, **15** and **17** were the most potent inhibitors of HIV-1 replication against HIV-1_{IIIB}, the EC_{50} ranged from 15 to 25 µM (SI value 10 to 28) and against HIV-1_{Ada} 5, the EC_{50} ranged from 15 to 64 µM (SI value 7 to 15.08). The other compounds **6**, **7**, **10** and **16**, also showed reasonable anti-HIV-1 potency: the EC_{50} ranged from 1-65 µM and 1-40 µM against HIV-1_{IIIB} and HIV-1_{Ada5} strains, respectively. The compounds having activity against HIV-1_{IIIB} and/or HIV-1_{Ada5} strains were taken for further anti-HIV-1 screening against the primary HIV-1 isolates from Uganda (HIV-1_{UG070}) and Indian (HIV-1_{VB59}) origin. The compounds **14**, **16** and **17** were found most active against primary isolates (EC_{50}: 5 to 35 µM; SI: 6.28 to 38.39 against HIV-1_{UG070} strain, EC_{50}: 25 to 98 µM; SI 4.97 to 8.06 against HIV-1_{VB59} strain) as shown in **Table 3**. Thus, in the cell based assay, amongst the 13 compounds the highest inhibitory activity was shown by compounds **14**, **15**, **16** and **17** with SI ranging between 4.96-28.04 against lab adapted strains, and with SI 2.31–38.39 against primary isolates. While the other compounds were moderate inhibitors of HIV-1 replication against HIV-1_{IIIB} and HIV-1_{Ada5} strains.

In view of the results obtained against HIV-1 using the strains HIV-1_{IIIB}, HIV-1_{Ada5} and primary isolates HIV-1_{UG070} and HIV-1_{VB59} from Uganda and Indian, respectively, under *in vitro* condition, we can conclude that the molecules acted as HIV-1 reverse transcriptase inhibitors and that the chemical skeletons of compounds **14**, **15**, **16** and **17** may be developed as lead HIV-1 RT inhibitors with suitable structure/ pharmacophore modifications. Further results in this direction will be described as separate studies.

Conflict of Interest: The authors declare no conflict of interest.

References

1. Global Report- UNAIDS report on the global AIDS epidemic, 2013.
2. Kumari G., Singh R. K., (2013) Anti-HIV drug development: structural features and limitations of present day drugs and future challenges in the successful HIV/AIDS treatment. Curr. Pharm. Des; 19: 1767-1783.
3. Kumari G., Singh R. K., (2012) Highly active antiretroviral therapy for treatment of HIV/AIDS patients: current status and future prospects and the Indian scenario, HIV & AIDS Review; 1:1 5-14.
4. De Clercq E. (2009) Anti-HIV drugs: 25 compounds approved within years after the discovery of HIV. Int. J. Antimicrob. Agents; 33: 307–320.
5. Jonckheere H., Anne J., De Clercq E. (2000) The HIV-1 reverse transcriptase (RT) process as target for RT inhibitors. Med. Res. Rev; 20: 129–154.
6. Singh R. K., Yadav D., Rai D., Kumari G., Pannecouque C. (2010) Synthesis, structure- activity relationship and antiviral activity of 3'-N, N-dimethylamino-2', 3'-dideoxythymidine and its prodrugs. Eur J. Med. Chem; 45: 3787-3793.
7. Drake S. M. (2000) NNRTIs- A new class of drugs for HIV. J. Antimicrob. Chemother; 45: 417–420.
8. Kumari G., Nutan, Modi M., Gupta S. K., Singh R. K. (2011) Rhodium (II) acetate-catalyzed stereoselective synthesis, SAR and anti-HIV activity of novel oxindoles bearing cyclopropane ring. Eur. J. Med. Chem; 46: 1181-1188.
9. Singh U. P., Singh R. K. (2011) Molecular docking analysis of novel non-nucleoside reverse transcriptase inhibitor in development: implication for rational drug design. Retrovirology; 8: 82.
10. Wang Z., Vince R. (2008) Synthesis of pyrimidine and quinolone conjugates as a scaffold for dual inhibitors of HIV reverse transcriptase and integrase. Bioorg Med Chem Lett; 18: 1293–1296.
11. Zhan P., Dongyue L., Junyi L., Xuwang C., Xinyong L., (2012) Benzimidazole heterocycle as a privileged scaffold in antiviral. Mini-Reviews in Organic Chemistry; 9: 397-410.
12. Peng Z., Xuwang C., Dongyue L., Zengjun F., De Clercq E., Xinyong L. (2013) HIV-1 NNRTIs: structural diversity, pharmacophore similarity, and impliations for drug design. 33: 1–72.
13. Lagos C.F., Caballero J., Gonzalez-Nilo F.D., Mahana D.P.C., Perez-Acle T. (2008) Docking and quantative structure-activity relationship studies for the Bisphenylbenzimidazole family of non-nucleoside inhibitors of HIV-1 reverse transcriptase. Chem Biol Drug Des; 72: 360–369.
14. Venkatachalam C.M., Jiang X., Oldfield T., Waldman M., (2003) LigandFit: a novel method for the shape- directed rapid docking of ligands to protein active sites. J. Mol. Graph. Model; 21: 289–307.
15. Hamdouchi C. et al. (2005) Structure-based design of a new class of highly selective aminoimidazo [1,2-a]pyridine-based inhibitors of cyclin dependent kinases. Bioorg. Med. Chem. Lett; 15: 1943-1947.
16. Bohm H.J. (1994) The development of a simple empirical scoring function to estimate the binding constant for a protein- ligand complex of known three-dimensional structure. J. Comput. Aided Mol. Des; 8: 243-256.
17. Bohm H.J. (1994) On the use of LUDI to search the Fine Chemicals Directory for ligands of proteins of known three-dimensional structure. J. Comput. Aided Mol. Des; 8: 623- 632.
18. Bohm H.J. (1998) Prediction of binding constants of protein ligands: a fast method for the prioritization of hits obtained from de novo design or 3D database search programs, J. Comput. Aided Mol. Des; 12; 309-323.
19. Wang R., Wang Y. Lu. S. (2003) Comparative evaluation of 11 scoring functions for molecular docking. J. Med. Chem; 46: 2287-303.
20. Prathipati P., Saxena A.K. (2006) Evaluation of binary QSAR models derived from LUDI and MOE scoring functions for structure based virtual screening. J. Chem. Inf. Model; 46: 39-51.
21. Patrick J. F., Neil J. G., Rachel F., Alan H. Brown T. (1996) Synthesis and properties of DNA–PNA chimeric oligomers. Nucleic Acids Research; 24: 3357–3363.
22. Rai D., Singh R. K. (2011) Synthesis and antibacterial activity of benzamides and sulfonamide derived from 2- amino-5-bromo/nitropyridine against bacterial strains isolated from clinical patients. Indian J. Chem; 50B: 931-936.
23. Parang K., Knaus E.E., Wiebe L.I. (1998) Synthesis, in vitro anti-HIV activity, and biological stability of 5'-O- myristoyl analogue derivatives of 3'-fluoro-2',3'-dideoxythymidine (FLT) as potential bifunctional prodrugs of FLT. Nucleosides & Nucleotides; 17: 987-1008.
24. Chen H., Lyne P.D., Giordanetto F., Lovell T., Li J. (2006) On evaluating molecular-docking Methods for pose prediction and enrichment factors; J. Chem. Inf. Model; 46: 401–415.
25. Gallivan J. P., Dougherty D. A. (1999) Cation-pi interactions in structural biology. Proc. Natl. Acad. Sci. USA; 96: 9459–9464.

26. Tang J., Maddali K., Dreis C. D., Sham Y. Y., Vince R., Pommier Y., Wang Z. (2011) N-3 Hydroxylation of Pyrimidine-2, 4-diones Yields Dual Inhibitors of HIV Reverse Transcriptase and Integrase. ACS Med. Chem. Lett; 2: 63–67.
27. Matthews B.W. (2001) Hydrophobic Interactions in Proteins University of Oregon, Eugene, Oregon, USA Encyclopedia of life sciences / & Nature Publishing Group / www.els.net).
28. Geonnotti, A. R.; Bilska, M.; Yuan, X.; Ochsenbauer, C.; Edmonds, T. G.; Kappes, J. C.; Liao, H. X.; Haynes, B. F.; Montefiori, D. C. Differential inhibition of human immunodeficiency virus type 1 in peripheral blood mononuclear cells and TZM-bl cells by endotoxin-mediated chemokine and gamma interferon production. *AIDS. Res. Hum. Retroviruses*. 2010, 26, 279.

Legends

Table 1 *N*-Heteroaryl Compounds 5-17 in the eyes of Lipinski's Rule

Table 2 Physical parameters, ligand score and stabilization energy of HIV-1 RT- ligand complexes of **5-17**

Table 3 Results of anti-HIV-1 activity, cytotoxicity and selectivity index in TZM-bl cells against HIV-1 lab adapted strains and primary isolates

Scheme1 Synthesis of compounds **5-13**

Reagents and conditions: i) H_2O, aq. KOH, 40 °C, 30 min; ii) CH_3CN / Py (v/v 3:1), oxalyl chloride, rt, 1h; iii) Py, Et_3N, 16 h

Scheme 2 Synthesis of compounds **14-17**

Reagents and conditions: i) CH_3CN / Py (v/v 3:1), Et_3N, rt, 12 h

Figure 1 **(A)** 'Butterfly conformation' of compound 17 showing hydrophobic character (shown by blue dots) **(B)**

Binding mode of compound **17** with HIV-1 RT: Stabilization of HIV-1 RT-ligand complex through hydrophobic interaction (surface view)

Figure 2 Hydrophobic interaction of compound **14-17** within HIV-1 RTwt NNIBP

Figure 3 Binding of compound **5-12** into allosteric site of HIV-1 RTwt (only surrounding residues are shown in grey, hydrogen bond shown by green dashed line and pi interaction shown by solid orange line)

Table 1

N-Heteroaryl Compounds 5-17 in the eyes of Lipinski's Rule

Compound	MW[1]	H-A[2]	H-D[3]	LogP[4]	TPSA[5]	violations
5	246	7	2	-1.029	96.85	0
6	325	7	2	-0.05	96.85	0
7	291	10	2	-0.9	142.68	0
8	260	7	2	-0.33	96.85	0
9	339	7	2	0.649	96.85	0
10	305	10	2	-0.201	142.68	0
11	252	5	1	1.401	59.81	0
12	331	5	1	2.38	59.82	0
13	297	8	1	1.53	105.64	0
14	428	6	2	2.62	83.98	0
15	360	12	2	0.92	175.62	1
16	318	6	0	2.97	69.79	0
17	408	12	0	2.80	161.44	1
Nevirapine	266.306	5	1	1.380	63.58	1
Etravirine	435.28	7	3	5.027	120.65	1

1. Molecular weight
2. number of H bond acceptors
3. number of H bond donors
4. Octanol-water partition coefficient
5. Total polar surface area

Table 2

Physical parameters, ligand score and stabilization energy of HIV-1 RT- ligand complexes of **5-17**

Compound	logP[1]	TPSA[2]	I.E[3]	Ludi_2[4]	ΔG_{pred}[5] (kcal/mol)	Ludi_3[4]	$_{P}EC_{50}$[6] (μM)	No. and amino acid in hydrogen bond	Distance (Aº)	No., type and amino acid in Pi bond	Distance (Aº)
5	-1.029	96.85	-40	284	-4.02	538	4.16×10^{-06}	0	--	2 'π- π' (Tyr181,Tyr318)	4.4, 4.5
6	-0.05	96.85	-41	409	-5.80	420	6.30×10^{-05}	2 (Lys103)	3.1, 3.0	--	--
7	-0.9	142.68	-43	335	-4.75	463	2.34×10^{-05}	2 (Lys103)	2.6, 2.7	--	--
8	-0.33	96.85	-41	389	-5.51	470	1.99×10^{-05}	1 (Lys103)	2.8	1 'π- π' (Phe227)	5.2
9	0.649	96.85	-44	426	-6.04	488	1.31×10^{-05}	2 (Val106, Tyr318)	3.2, 2.9	--	--
10	-0.201	142.68	-44	342	-4.85	407	8.51×10^{-05}	3 (Lys103, Tyr181)	2.8, 3.1,3.1	--	--
11	1.401	59.81	-38	354	-5.02	751	3.0×10^{-08}	--	--	2 'π- π' (Tyr181)	4.4, 5.3
12	2.38	59.82	-43	407	-5.77	423	5.88×10^{-05}	1 (Lys103)	2.8	--	--
13	1.53	105.64	-44	370	-6.04	426	5.49×10^{-05}	1 (Lys103)	2.8	--	--
14	2.62	83.98	-48	451	-6.39	460	2.51×10^{-05}	--	--	--	--
15	0.92	175.62	-52	401	-5.68	420	6.30×10^{-05}	--	--	--	--
16	2.97	69.79	-46	427	-6.05	694	1.14×10^{-07}	--	--	--	--

17	2.80	161.44	-53	328	-4.65	409	8.12×10^{-05}	--	--	--	--
Nevirapine	1.380	63.58	-45	393	-5.57	557	0.27×10^{-05}	--	--	2 'π- π' (Tyr181,Tyr188)	6.0, 5.1

1. Octanol-water partition coefficient
2. Total polar surface area
3. Total interaction energy
4. Ludi_2 and Ludi_3, empirical scoring functions derived from the Ludi algorithm
5. Predicted binding free energy
6. Predicted 50% effective concentration required to inhibit HIV1 replication

Table 3 Results of anti-HIV-1 activity, cytotoxicity and selectivity index in TZM-bl cells against HIV-1 lab adapted strains and primary isolates

Number of compound	Anti-HIV-1 activity[1] agains t HIV-1 lab adapted strains					Anti-HIV-1 activity[1] against primary isolates				
	EC_{50}[2] (μM)		CC_{50}[3] (μM)	SI[4]	SI[4]	EC_{50}[2] (μM)		CC_{50}[3] (μM)	SI[4]	SI[4]
	HIV-1 III_B	HIV-1 ADA5	TZM-bl cells	HIV-1 III_B	HIV-1 ADA5	HIV-1 UG070	HIV-1 VB59	TZM-bl cells	HIV-1 UG070	HIV-1 VB59
5	243	178	602	2.47	3.38	113	394	602	5.32	1.52
6	65	43	215	3.30	5	70	134	215	3.07	1.6
7	1	1.3	6.32	6.32	4.86	2.40	2.68	6.32	2.63	2.35
8	23	26	49	2.13	1.88	29.6	23.26	49	1.65	2.1
9	17	39.43	56.50	3.32	1.43	39.43	43.57	56.50	1.43	1.29
10	17.6	30.65	78.75	4.47	2.56	32.68	42.13	78.75	2.4	1.86
11	381	NA	541.98	1.42	NA	389	ND	542	1.39	ND
12	NA	76	118	ND	1.5	ND	NA	ND	ND	ND
13	6.7	9.59	18.14	2.7	1.89	8.65	NA	18.14	2.1	ND
14	28.03	63.08	487.6	17.39	7.73	35.04	98.13	487.6	13.91	4.97

15	15.7	58.33	442.5	28	7.59	110.5	191.6	442.5	4	2.31
16	40	40	202.8	4.96	4.96	5.28	25.15	202.8	38.39	8.06
17	17.1	15.4	184.77	10.77	15.08	29.41	31.86	184.7	6.28	5.8

1. Represents mean of two independent assay
2. EC_{50} is the 50% effective concentration required to inhibit HIV1 replication for strains IIIB, ADA5, UG070 and VB59 in the TZMbl cell line
3. CC_{50} is the 50% cytotoxic concentration of the respective compound to the TZMbl cells
4. Selectivity index ratio CC_{50}/ EC_{50}

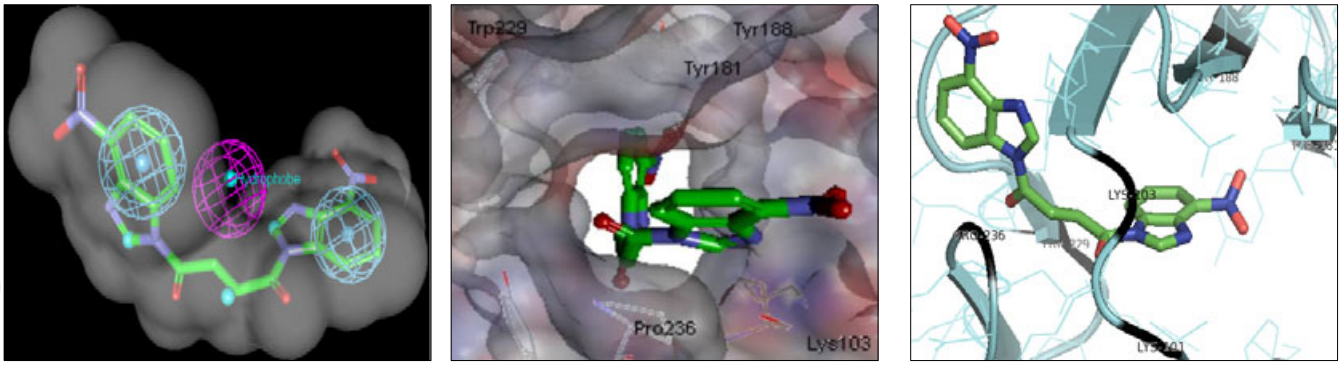

(A) **(B)** **(C)**

Figure 1 (A) 'Butterfly conformation' of compound **17** showing hydrophobic character (shown by blue dots) **(B)** Binding mode of compound **17** with HIV-1 RT: Stabilization of HIV-1 RT-ligand complex through hydrophobic interaction (surface view) **(C)** Docking results of **17** into NNIBP of HIV-1 RTwt

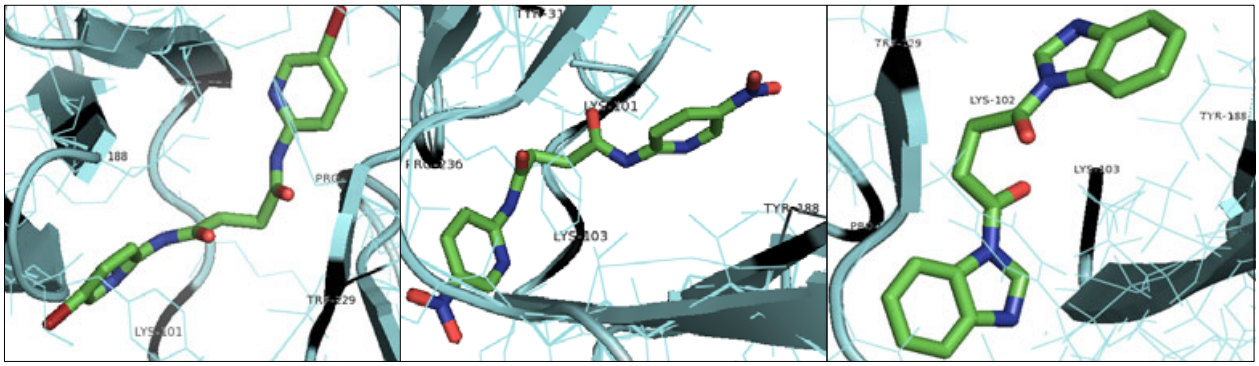

14 **15** 16

Figure 2 Hydrophobic interaction of compound **14-17** within NNIBP of HIV-1 RTwt

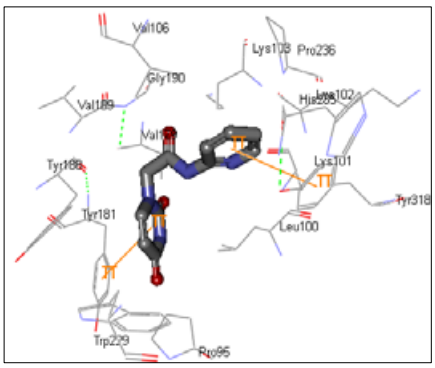

5

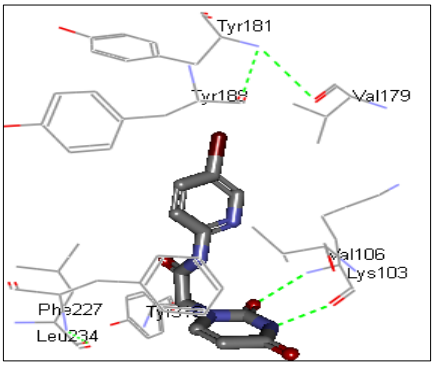

6

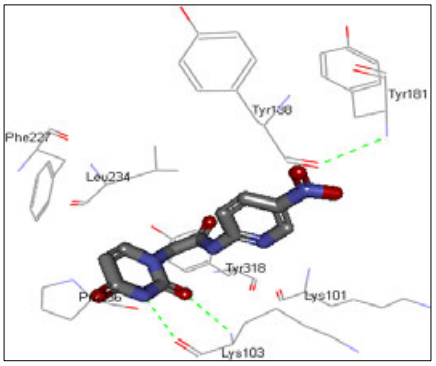

7

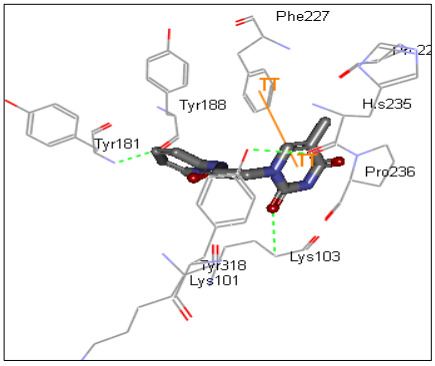

8

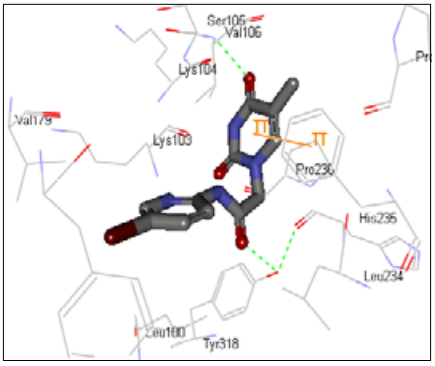

9

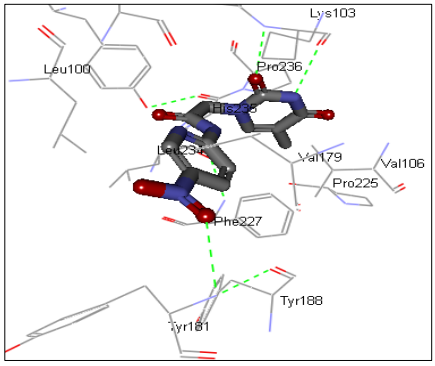

10

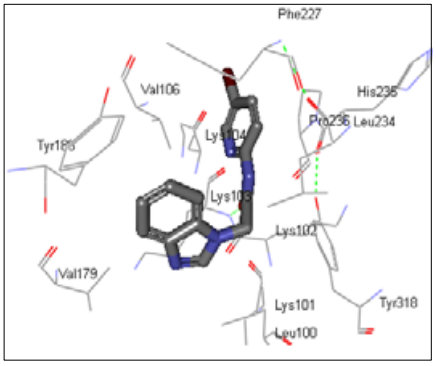

11

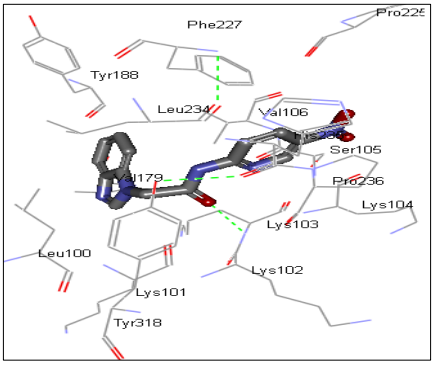

12

Figure 3 Binding of compound **5-12** into allosteric site of HIV-1 RTwt (only surrounding residues are shown in grey, hydrogen bond shown by green dashed line and pi interaction shown by solid orange line)

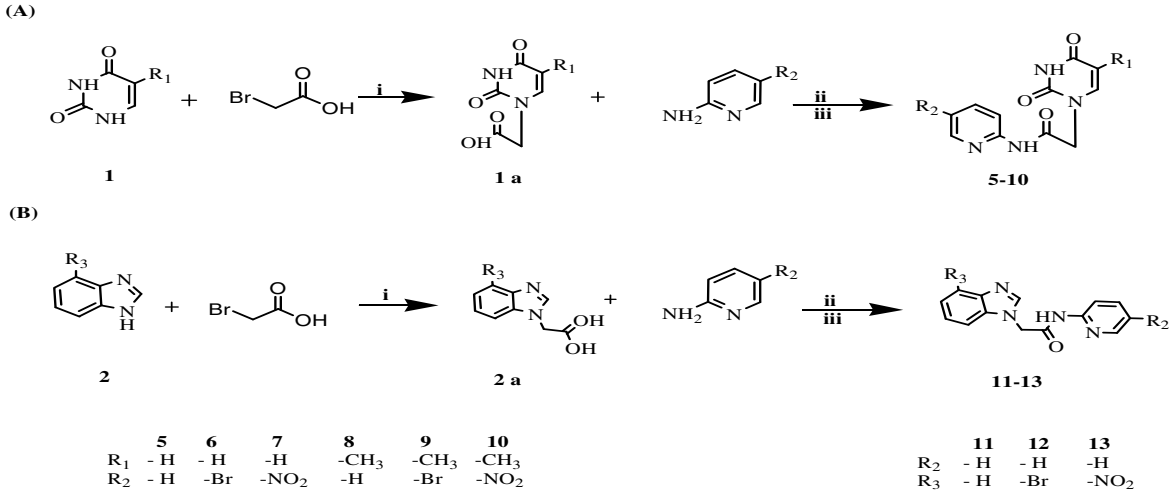

Scheme 1 Synthesis of compounds **5-13**
Reagents and conditions: i) H_2O, aq. KOH, 40 °C, 30 min; ii) CH_3CN / Py (v/v 3:1), oxalyl chloride, rt, 1h; iii) Py, Et_3N, 16 h

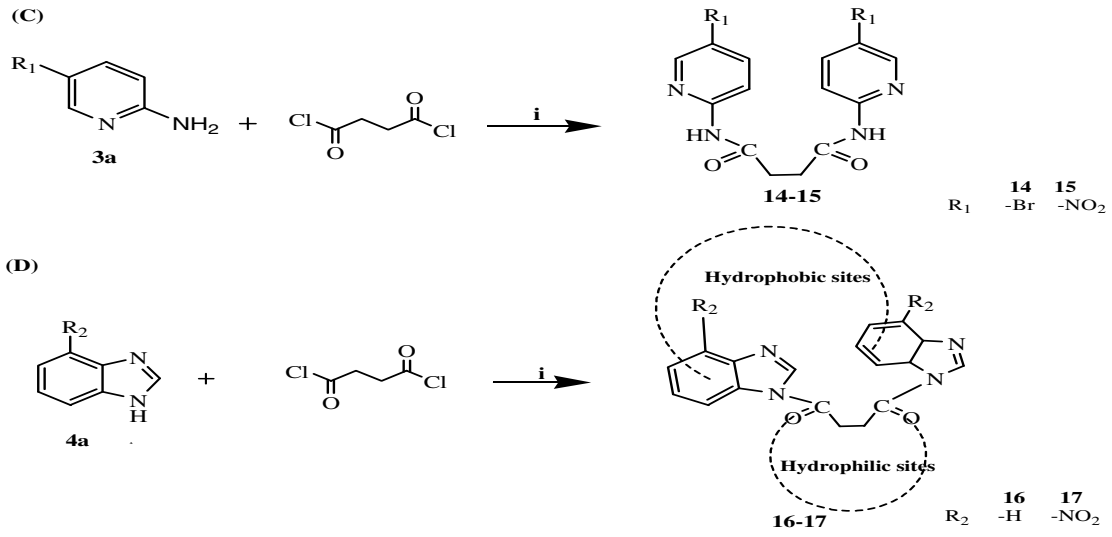

Scheme 2 Synthesis of compounds **14-17**
Reagents and conditions: i) CH_3CN / Py (v/v 3:1), Et_3N, rt, 12 h